


The Augmentation of a Collagen/Glycosaminoglycan Biphasic Osteochondral Scaffold with Platelet-Rich Plasma and Concentrated Bone Marrow Aspirate for Osteochondral Defect Repair in Sheep: A Pilot Study

Cartilage
3(4) 351–363
© The Author(s) 2012
Reprints and permission:
sagepub.com/journalsPermissions.nav
DOI: 10.1177/1947603512444597
http://cart.sagepub.com


Alan Getgood¹, Frances Henson², Carrie Skelton³, Emilio Herrera⁴, Roger Brooks³, Lisa A. Fortier⁵, and Neil Rushton³

Abstract

Objective: This study investigates the combination of platelet-rich plasma (PRP) or concentrated bone marrow aspirate (CBMA) with a biphasic collagen/glycosaminoglycan (GAG) osteochondral scaffold for the treatment of osteochondral defects in sheep. **Design:** Acute osteochondral defects were created in the medial femoral condyle (MFC) and the lateral trochlea sulcus (LTS) of 24 sheep ($n = 6$). Defects were left empty or filled with a 6×6 -mm scaffold, either on its own or in combination with PRP or CBMA. Outcome measures at 6 months included mechanical testing, International Cartilage Repair Society (ICRS) repair score, modified O'Driscoll histology score, qualitative histology, and immunohistochemistry for type I, II, and VI collagen. **Results:** No differences in mechanical properties, ICRS repair score, or modified O'Driscoll score were detected between the 4 groups. However, qualitative assessments of the histological architecture, Safranin O content, and collagen immunohistochemistry indicated that in the PRP/scaffold groups, there was a more hyaline cartilage-like tissue repair. In addition, the addition of CBMA and PRP to the scaffold reduced cyst formation in the subchondral bone of healed lesions. **Conclusion:** There was more hyaline cartilage-like tissue formed in the PRP/scaffold group and less subchondral cystic lesion formation in the CBMA and PRP/scaffold groups, although there were no quantitative differences in the repair tissue formed.

Keywords

cartilage repair, osteochondral scaffold, platelet rich plasma

Introduction

Articular cartilage has a limited ability to regenerate following injury. Many different surgical procedures are in routine use worldwide in order to promote cartilage and subchondral bone healing,¹ such as microfracture,² autologous chondrocyte transplantation,³ and mosaicplasty.⁴ However, while these techniques are widely used in clinical practice, research continues into other improved repair methods.⁵ Recently, a greater emphasis has been placed on the role of the subchondral bone and its influence on clinical presentation and disease progression,⁶ and as a result, many new repair techniques incorporate regeneration of the osteochondral unit.

Recent advances in biomaterials have led to the production of a number of biosynthetic scaffolds for use in chondral

and osteochondral repair.⁷ The aims of using such scaffolds are to mimic the 3-dimensional environment of the extracellular matrix (ECM), provide structural support to the regenerated and surrounding tissues, and provide an increased surface area to volume ratio for cellular infiltrate

¹Fowler Kennedy Sport Medicine Clinic, University of Western Ontario, London, Ontario, Canada.

²Department of Veterinary Medicine, University of Cambridge, Cambridge, UK

³Orthopaedic Research Unit, University of Cambridge, Cambridge, UK

⁴Department of Physiology, University of Cambridge, Cambridge, UK

⁵Cornell University, Ithaca, NY, USA

Corresponding Author:

Alan Getgood, Fowler Kennedy Sport Medicine Clinic, 3M Centre, University of Western Ontario, London, Ontario, N6A 3K7.
Email: agetgood@btinternet.com

and colonization. In osteochondral defects, it has been proposed that multiphasic scaffolds are required for optimal tissue repair as the cartilage and bone have different requirements for optimal healing.⁸

ChondroMimetic (TiGenix, Cambridge, UK) is a novel, biological biphasic osteochondral scaffold licensed for osteochondral repair in Europe. It is based upon the collagen/glycosaminoglycan (collagen-GAG) platform technology developed over 30 years ago.^{9,10} It is comprised of an unmineralized bovine type I collagen/GAG (chondroitin-6-sulfate) "chondral" layer coupled to a bovine type I collagen/GAG "osseous" layer, mineralized with calcium phosphate in its brushite phase. A preliminary caprine *in vivo* study has indicated that this scaffold can support osteochondral healing and cartilage regeneration when used alone, which have led to it being licensed for use in clinical practice.¹¹

The physical properties of biosynthetic scaffolds often permit them to be used as carrier vehicles for the delivery of biological factors into the osteochondral defect site, which may affect tissue healing. Many biological factors have been reported to promote osteochondral tissue repair and regeneration. Clinically, the use of autologous products, such as bone marrow aspirate or platelet-rich plasma (PRP), rather than commercially available recombinant proteins, has many advantages including the lack of an antigenic response, the ease of availability of the source material, and the relative low costs. One of the most commonly used autologous cellular products in tissue engineering is the bone marrow-derived mesenchymal stem cell (BMSC),¹² which is found in concentrated bone marrow aspirate (CBMA). BMSCs are multipotent cells that differentiate into chondrocytes under certain culture conditions, including the application of growth factors such as fibroblast growth factor 2 (FGF-2) and transforming growth factor beta 1 and 3 (TGF- β 1/TGF- β 3).¹³ BMSCs have been used in a number of *in vivo* osteochondral repair models^{14,15} and have been shown to have beneficial effects on tissue repair.

PRP is another autologous product that has generated significant interest for tissue repair.¹⁶ Platelets are a rich source of a number of growth factors including platelet-derived growth factor (PDGF), TGF- β 1, and FGF-2.¹⁷ A number of studies have shown that platelet concentrates affect processes involved in both bone repair (including osteoblast differentiation, angiogenesis, and bone marrow cell recruitment)^{18,19} and chondrocyte metabolism and behavior (including enhancing chondrocyte proliferation and matrix protein synthesis).^{20,21} These results suggest a possible role for PRP in osteochondral repair. Recent work done in our group has demonstrated the ability of the collagen-GAG biphasic scaffold to support significant growth factor release from the PRP,²² making its use in combination with the collagen-GAG scaffold a possible route by which to deliver autologous growth factor into the repair site.

The purpose of this study was to investigate whether the addition of CBMA (a source of BMSC) or PRP to a collagen-GAG scaffold at the point of service, that is, the operating theater, would have a positive impact on tissue repair in an acute ovine osteochondral defect model.

Materials and Methods

This study received approval from both the local research ethics committee and the Home Office.

Animals

A total of 24 skeletally mature Welsh Mountain sheep (mean age = 4.3 years) were included in the study. Each treatment group contained 6 sheep.

Experimental Design

For all animals, full-thickness osteochondral defects, 5.8-mm wide by 6-mm deep, were created in the proximal lateral trochlea sulcus (LTS) and in the medial femoral condyle (MFC) of the right stifle joint using custom-made instrumentation. Four treatment groups were created. The first group ($n = 6$) had no scaffold placed into the defects (empty), and the second group ($n = 6$) was filled with scaffold alone (scaffold only). The third group ($n = 6$) of animals had the defects filled with scaffold plus CBMA (scaffold + CBMA) and the fourth group ($n = 6$) with scaffold plus PRP (scaffold + PRP).

Animal Anesthesia, Preparation, and Surgical Technique

Prior to surgery, animals were selected at random and identification ear tags applied. All animals had food and water removed 24 hours before surgery. General anesthesia was induced with an injection of thiopentone (3 mg/kg) into the external jugular vein. Maintenance was achieved via inhalational anesthetic of a mixture of isoflurane, nitrous oxide, and oxygen. Perioperative analgesia was provided by preoperative intramuscular carprofen (1.5 mg/mL), and antibiotic prophylaxis was also given via intramuscular procaine penicillin (10 mg/mL).

The basic surgical procedure was identical for all subjects and performed under strict asepsis by a single surgeon. Each stifle was physically examined for any abnormalities while anesthetized. If any gross instability or pathology was found, the animal was excluded from participation within the study.

The animal was placed in a dorsal recumbent position and, following surgical preparation, the right stifle joint opened via a lateral parapatellar approach. Following patellar subluxation, the LTS defect was made 10 mm distal to

Table 1. Cell Counts in Whole Blood (WB) and Platelet-Rich Plasma (PRP) ($\times 10^3/L$), with the Corresponding Concentration Factor (X)

Sheep ID	Platelet WB	Platelet PRP	X	WBC WB	WBC PRP	X	Monocyte WB	Monocyte PRP	X
B19	39.9	1353	33.9	5.58	37.6	6.7	0.13	1.43	11.0
B20	39.4	742	18.8	7.08	93.4	13.2	0.256	16.6	64.8
B22	53.5	210	3.9	16.6	16.2	1.0	0.715	0.741	1.0
B26	214	1158	5.4	4.63	84.4	18.2	0.041	1.58	38.5
B34	205	937	4.6	5.01	47.5	9.5	0.541	0.427	0.8
B35	144	3634	25.2	7.47	92.4	12.4	0.115	3.69	32.1

Note: WBC = white blood cell.

the top of the lateral trochlear ridge aligned with the middle of the lateral trochlear groove. The MFC defect was made 10 mm distal to the condyle groove junction and aligned with the medial crest of the trochlear groove. A 5.8-mm-wide \times 6-mm-deep circular defect was created and the scaffold plus appropriate test substance placed into the defect. The joint was then cycled through a range of motion to ensure a satisfactory rim fixation of the plug. The joint was closed in a standard fashion. No splints, casts, or immobilization techniques were used in any animal.

Postoperatively, animals were allowed to fully bear weight but kept in small pens for 48 hours to reduce ambulation. All animals were housed indoors for the remaining study period in large pens, which allowed a moderate degree of ambulation. Regular checks were made for any animal displaying signs of postoperative discomfort, with additional postoperative analgesia given if required. All further treatments were recorded as appropriate. The surgical procedures and recovery from surgery were uneventful.

PRP Preparation

Following anesthesia, 60 mL of peripheral blood was aspirated from the external jugular vein into 6 mL of acid-citrate-dextrose anticoagulant and PRP prepared using the SmartPRP 2 system (Harvest Technologies, Plymouth, MA). A modified protocol to that recommended by the manufacturers for human blood was established during preliminary experiments. This consisted of adding an extra 220-second spin cycle centrifugation step to the protocol to allow maximal separation of the ovine erythrocytes and platelets, which was validated prior to beginning the experiment. Platelet, white blood cell (WBC), and monocyte numbers were measured in all of the PRP constructs produced. Platelets were concentrated between 3.9 and 33.9 times, WBCs were concentrated between 1 and 18.2 times, and monocytes were concentrated between 0.8 and 38.5 times (Table 1).

CBMA

Bone marrow aspirates were taken from the posterior iliac crests via 11-gauge Jamshidi bone marrow harvest needles

Table 2. Cell Counts of Bone Marrow Aspirate Following Density Centrifugation ($\times 10^9/L$)

Sheep ID	Total nucleated cell	Mononuclear cell
B23	0.25	0.1
B24	3.55	1.7
B25	2.15	0.8
B27	4.33	2.22
B28	6.87	1.8
B30	6.65	3.45

following induction of general anesthesia and prior to defect production. A maximum of 20 mL of bone marrow was aspirated from each iliac crest into 1,000 U of heparin. A bone marrow concentrate was then produced using density gradient centrifugation. The bone marrow sample was diluted with 20 mL of sterile phosphate buffered saline and the mixture layered onto equal volumes of Lymphoprep (Axis-Shield, Oslo, Norway) density gradient medium and centrifuged at 900g for 20 minutes. The buffy layer incorporating the mononuclear cells was then removed and a cell pellet produced via further centrifugation at 750g for 10 minutes. The resulting cell pellet was reconstituted with 500 μ L of DMEM/F12 medium. A volume of 200 μ L was added to each scaffold and the rest of the suspension used to obtain a cell number and percentage of viability using trypan blue. The bone marrow cell counts, which included all nucleated cells, were measured for all animals and ranged from 0.25 to $6.87 \times 10^9/L$ (Table 2). All were found to have cell viabilities greater than 95% following density centrifugation.

Necropsy

Animals were humanely sacrificed at 26 weeks postoperatively using a lethal dose of sodium pentobarbital.

Gross Morphology

The joints were opened and photographed and the surface of the osteochondral defect sites blindly scored (F.H.) using the International Cartilage Repair Society (ICRS) score (Table 3). Two animals, both in the empty defect control

Table 3. Scoring Criteria Using the International Cartilage Repair Society Score to Assess the Integration of the Scaffold into the Joint

Characteristic	Grading	Score
Degree of defect repair	Level with surrounding cartilage	4
	75% repair of defect depth	3
	50% repair of defect depth	2
	25% repair of defect depth	1
	0% repair of defect depth	0
Integration to border zone	Complete integration with border zone	4
	Demarcating border <1 mm	3
	¾ of graft integrated, ¼ with notable border >1 mm	2
	½ of graft integrated with surrounding cartilage, ½ with a notable border >1 mm	1
	From no contact to ¼th of graft integrated with surrounding cartilage	0
Macroscopic appearance	Intact smooth surface	4
	Fibrillated surface	
	Small, scattered fissures or cracks	3
	Several small or few but large fissures	2
	Total degeneration of grafted area	1
Total		12

group, were excluded from the study at postmortem, one due to a small fracture of the lateral trochlear ridge extending into the defect and the second due to a chronically subluxed patella, which would have caused altered biomechanics of the affected stifle joint. Both were deemed to influence the resultant tissue repair, hence their exclusion.

Mechanical Testing

After the gross morphological observations were made, each implant site underwent nondestructive mechanical testing to determine changes to the cartilage surface surrounding the implant or empty defect. Stiffness measurements were taken in duplicate from the center of the osteochondral defect and at a distance of 1 mm from the original edge of the created osteochondral defect at the 12-, 3-, 6-, and 9-o'clock positions and 1 mm from the edge in the perilesional cartilage, using a handheld digital durometer (Shore S1, M scale, Instron, Norwood, MA). A number between 0 and 100 would be given with a built-in calibrated error of ± 5 . These measurements were then repeated in the contralateral limb in the same anatomic sites. The stiffness of the reparative tissue was then expressed as a percentage

of stiffness relative to the control cartilage of the contralateral limb and the perilesional cartilage of the ipsilateral limb.

Histology

Following stiffness measurements, the specimens were decalcified in formic acid/sodium citrate over 2 weeks. Following complete decalcification, the specimens were dehydrated through a series of ethanol exchanges of increasing concentrations and then embedded in paraffin wax. Sections of 10- μ m thickness were made through the central portion of the defect. Sections were stained with Safranin O/Fast Green. The histology sections were blindly scored by one investigator (F.H.), using a modified O'Driscoll score (Table 4).²³

Correction of O'Driscoll Scores for PRP and CBMA Values

Given the wide range of CBMA and platelet concentrations within each experimental group, further analysis of the histological data was performed. Correlations between the O'Driscoll scores and the cell concentrations and total cell numbers were evaluated.

Immunohistochemistry

Immunohistochemistry was performed as described previously.²⁴ The following primary antibodies were used in this study: monoclonal mouse anti-human type I collagen (1:200 dilution, MP Biomedicals, Solon, OH), monoclonal mouse anti-human type II collagen (1:100 dilution, MP Biomedicals), and monoclonal mouse anti-rabbit type VI collagen (1:500 dilution, Abcam, Cambridge, UK). Horseradish peroxidase-conjugated secondary anti-rabbit and mouse immunoglobulins were used as appropriate and the color reaction developed with 0.1% 3',3'-diaminobenzidine tetrachloride (DAB)/0.01% hydrogen peroxide. Normal species-specific serum was used as a control in all experiments.

The degree of positive staining for type I, II, and VI collagens was evaluated by semiquantitative scoring on a scale of 1 to 4 for intensity, that is, inconspicuous (1), mild (2), moderate (3), and strong (4).²⁴ In addition, the location of type VI immunoreactivity was noted, that is, pericellular or territorial.

Statistical Analysis

Statistical significance between groups and within groups for each end point was determined using a 1-way analysis of variance (ANOVA) and Bonferroni *post hoc* test. Where data sets within groups were not found to be normally distributed, a nonparametric Kruskal-Wallis test was instead

Table 4. Modified O'Driscoll Histology Score

Characteristic	Grading	Score
I. Hyaline cartilage	80%-100%	8
	60%-80%	6
	40%-60%	4
	20%-40%	2
	0%-20%	0
II. Structural characteristics		
A. Surface irregularity	Smooth and intact	2
	Fissures	1
	Severe disruption, fibrillation	0
B. Structural integrity	Normal	2
	Slight disruption, including cysts	1
C. Thickness	Severe lack of integration	0
	100% of normal adjacent cartilage	2
	50%-100% or thicker than normal	1
D. Bonding to adjacent cartilage	0%-50%	0
	Bonded at both ends of graft	2
	Bonded at one end/partially both ends	1
III. Freedom from cellular changes of degeneration	Not bonded	0
	Normal cellularity, no clusters	2
	Slight hypocellularity, <25% chondrocyte clusters	1
IV. Freedom from degenerate changes in adjacent cartilage	Moderate hypocellularity, >25% clusters	0
	Normal cellularity, no clusters, normal staining	3
	Normal cellularity, mild clusters, moderate staining	2
V. Reconstitution of subchondral bone	Mild or moderate hypocellularity, slight staining	1
	Severe hypocellularity, slight staining	0
	Complete reconstitution	2
VI. Bonding of repair cartilage to <i>de novo</i> subchondral bone	>50% reconstitution	1
	≤50% reconstitution	0
	Complete and uninterrupted	2
VII. Safranin O staining	<100% but >50% reconstitution	1
	<50% complete	0
	>80% homogenous positive stain	2
Total score	40%-80% homogenous positive stain	1
	<40% homogenous positive stain	0
		Max. 27

used, with a *post hoc* Dunn multiple comparison test. A level of $P < 0.05$ was accepted as significant in all analyses. Correlation coefficients were calculated by plotting concentration factors against histology scores and a best-fit line produced with corresponding R^2 value. GraphPad Prism 5 statistical software package (GraphPad Software Inc., La Jolla, CA) was used for data analysis.

Results

Gross Morphology

The quality of repair at the site of the defect was assessed using the ICRS scale. **Figure 1** shows the distribution of mean scores between experimental groups. A trend towards an increase in ICRS score is seen with the scaffold + PRP and scaffold + CBMA groups compared to the empty defects and scaffold alone, but no statistically significant difference existed between groups ($P = 0.619$).

Mechanical Testing (Tables 5 and 6)

All treatment groups in the MFC and LTS were found to have similar mean stiffness measurements compared to the contralateral limb and perilesional cartilage ($P > 0.05$). However, there was a trend toward increasing stiffness seen in the empty defects in both the LTS and MFC.

Quantitative Histology

Modified O'Driscoll histology scores (Fig. 2). A trend towards an increased O'Driscoll score was noted in the scaffold + PRP group compared to the other 3 treatment groups, particularly in the MFC, but this was not statistically significant ($P = 0.097$).

A negative correlation was found between the PRP platelet concentration factor and resultant O'Driscoll histology score in the LTS ($R^2 = 0.74$). No other correlation was found between total white cell concentration, monocyte concentration, or CBMA cell count versus O'Driscoll score.

Qualitative Cartilage Histology

Tissue fill (Figs. 3 and 4). In the empty defect, scaffold only, and scaffold + CBMA defects, the thickness of the cartilage repair tissue was less than the thickness of the normal adjacent cartilage. In the scaffold + PRP defects, the cartilage thickness was restored to nearly normal.

Residual scaffold and the formation of cystic lesions were noted in the tissue filling the subchondral bone region at both anatomic sites. However, there were clear differences in the detection of residual scaffold and the appearance of cysts between the treatment groups. At both sites, there was a reduction in the appearance of residual scaffold

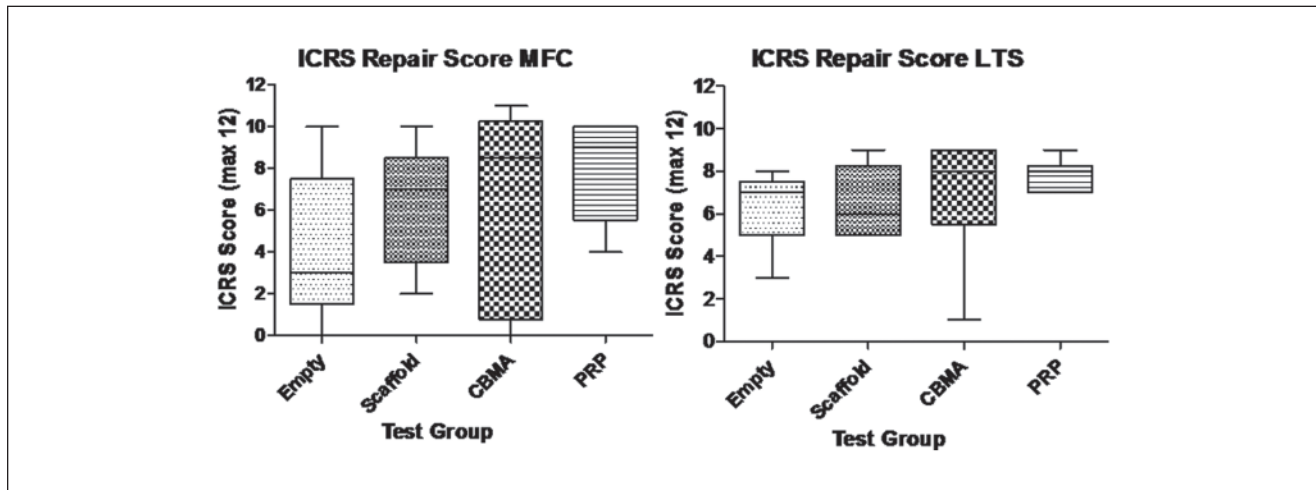


Figure 1. Mean ICRS scores for empty osteochondral defects (Empty), osteochondral defects filled with ChondroMimetic scaffold (Scaffold), osteochondral defects filled with ChondroMimetic scaffold loaded with concentrated bone marrow aspirate cells (CBMA), and osteochondral defects filled with ChondroMimetic scaffold loaded with platelet-rich plasma (PRP). Data are presented for defects in both the medial femoral condyle (MFC) and the lateral trochlea sulcus (LTS). In neither the MFC or the LTS is there a statistically significant difference between the 4 treatment groups.

Table 5. Summary Data for the Mechanical Stiffness of the Repair Cartilage Expressed as a Percentage of the Contralateral Limb Cartilage

	Empty defect		Scaffold only		CBMA		PRP	
	MFC	LTS	MFC	LTS	MFC	LTS	MFC	LTS
Mean	126.4	85.4	97.2	79.3	97.6	81.1	102.1	82.5
Standard deviation	66.8	13.8	13.8	8.1	25.6	17.7	17.2	11.4
Standard error	29.9	6.2	5.6	3.3	10.5	7.2	7.0	4.7
Lower 95% CI	43.5	68.3	82.7	70.9	70.7	62.5	84.0	70.5
Upper 95% CI	209.3	102.5	111.7	87.8	124.4	99.7	120.2	94.4

$P < 0.05$

Note: CBMA = concentrated bone marrow aspirate; PRP = platelet-rich plasma; MFC = medial femoral condyle; LTS = lateral trochlea sulcus; CI = confidence interval.

Table 6. Summary Data for the Mechanical Stiffness of the Repair Cartilage Expressed as a Percentage of the Perilesional Cartilage

	Empty defect		Scaffold only		CBMA		PRP	
	MFC	LTS	MFC	LTS	MFC	LTS	MFC	LTS
Mean	104.9	92.0	97.3	87.3	111.9	86.1	98.0	86.7
Standard deviation	16.9	4.9	11.4	12.2	30.3	21.0	10.9	11.7
Standard error	7.6	2.2	4.6	5.0	12.4	8.6	4.4	4.8
Lower 95% CI	83.8	85.9	85.3	74.6	80.1	64.1	86.6	74.5
Upper 95% CI	125.9	98.0	109.2	100.1	143.6	108.2	109.4	99.0

$P < 0.05$

Note: CBMA = concentrated bone marrow aspirate; PRP = platelet-rich plasma; MFC = medial femoral condyle; LTS = lateral trochlea sulcus; CI = confidence interval.

in the scaffold + CBMA group compared to the other groups, and cysts were only detected in the control and control + scaffold groups; 22% of sections from the empty or scaffold only groups had cysts compared to none in the scaffold + PRP or scaffold + CBMA groups.

Safranin O staining (Fig. 3). In the empty defects, positive Safranin O staining was seen in the repair tissue in all MFC empty defects, with relatively poor staining in the LTS empty defects. In the defects that had been filled with scaffold only and scaffold + CBMA, there was moderate

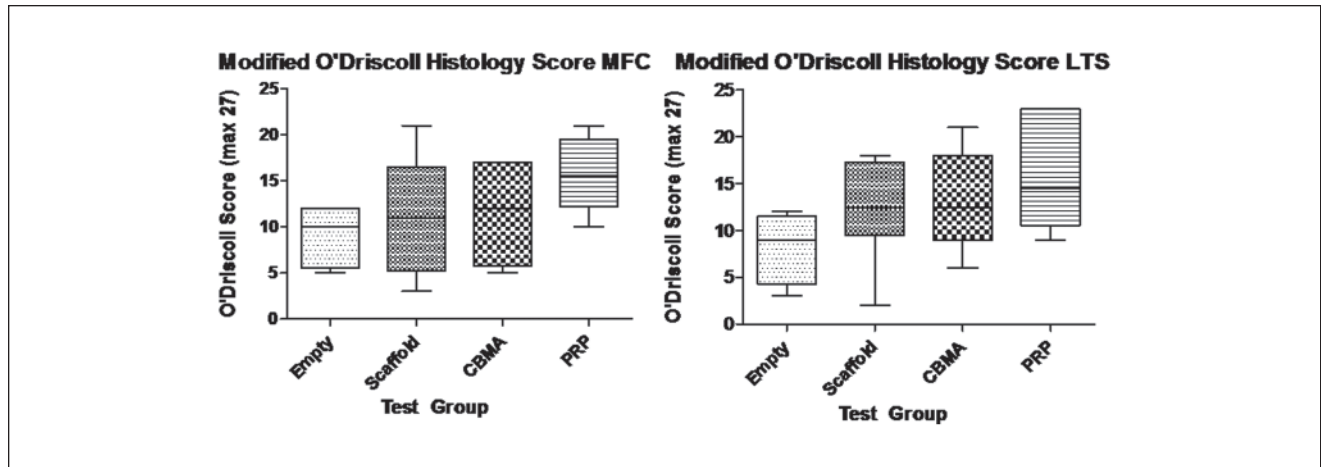


Figure 2. Modified O'Driscoll histology scores for empty osteochondral defects (Empty), osteochondral defects filled with ChondroMimetic scaffold (Scaffold), osteochondral defects filled with ChondroMimetic scaffold loaded with concentrated bone marrow aspirate cells (CBMA), and osteochondral defects filled with ChondroMimetic scaffold loaded with platelet-rich plasma (PRP). Data are presented for defects in both the medial femoral condyle (MFC) and the lateral trochlea sulcus (LTS). In neither the MFC or the LTS is there a statistically significant difference between the 4 treatment groups, although there is a strong trend towards an increased score in the scaffold/PRP defects compared to the empty defects.

staining in all sections. In the scaffold + PRP sections, there was strong Safranin O staining, indicating high proteoglycan content within the repair tissue.

Cellular organization (Fig. 3). In empty defects, there was little evidence of organized repair tissue; however, in scaffold-filled defects, there was some evidence of more organized tissue being produced. In the MFC of scaffold only defects, chondrocytes were seen in lacunae arranged in columns in the deep zone, with more flattened chondrocytes in the superficial zone. This was seen mostly in the lateral margins, with more disorganized tissue often found centrally. In the CBMA group, disorganized cellular organization was seen, particularly centrally. In contrast, in the scaffold + PRP defects, there were rounded cells orientated in a columnar fashion, within lacunae, in the deep and middle zones, becoming more flattened closer to the superficial layer.

Collagen immunohistochemistry (Figs. 5 and 6). All empty defect repair tissue showed positive type I collagen staining with no pericellular type VI collagen staining and little type II collagen staining, indicating a fibrocartilage tissue fill. In defects filled with scaffold only, the repair tissue demonstrated both type I and II collagen staining with pericellular type VI staining in the lateral margins of the repair tissue, indicating a mixed hyaline/fibrocartilage repair. In the scaffold + CBMA group, both LTS and MFC defects showed good type II collagen staining and reduced type I collagen staining compared to the scaffold only treatments, with pericellular type VI collagen present at the margins of the MFC defect. In the scaffold + PRP defects, there was strong type II collagen staining with mild type I staining. In the MFC defect, pericellular type VI collagen was detected throughout the repair zone. These results, combined with

the Safranin O staining and cellular organization, would suggest that scaffold + PRP produce repair tissue with more characteristics of hyaline cartilage.

Discussion

Autologous products such as CBMA and PRP are readily available biological factors, which can easily be delivered into osteochondral defects carried by biosynthetic scaffolds. Both CBMA and PRP are currently "fashionable" treatments and are being used to treat many orthopedic conditions. In this pilot study, we have examined the effect of the addition of CBMA and PRP to a biphasic scaffold in the treatment of an acute ovine osteochondral injury model but have shown no statistically significant improvement in any of the quantitative end points studied. There was no significant difference noted in the gross cartilage repair score, the mechanical stiffness of the defects between groups, or the quantitative histology score of the repairing cartilage. Qualitative assessment of the repair tissue with Safranin O, assessment of the architecture of the cartilage produced, and immunohistochemistry staining suggested that repair tissue with more features of hyaline cartilage was produced in the scaffold + PRP group over the other treatment groups. This was assessed by observing an increase in type II collagen and reduction in type I collagen immunohistochemical staining in these sections, with pericellular type VI collagen staining of the cells throughout the chondral repair tissue, which has been proposed to indicate a mature chondrocyte phenotype.²⁵ These findings, in combination with the strong positive Safranin O staining indicating proteoglycan deposition within the ECM, and rounded chondrocytes with zonal organization, would be

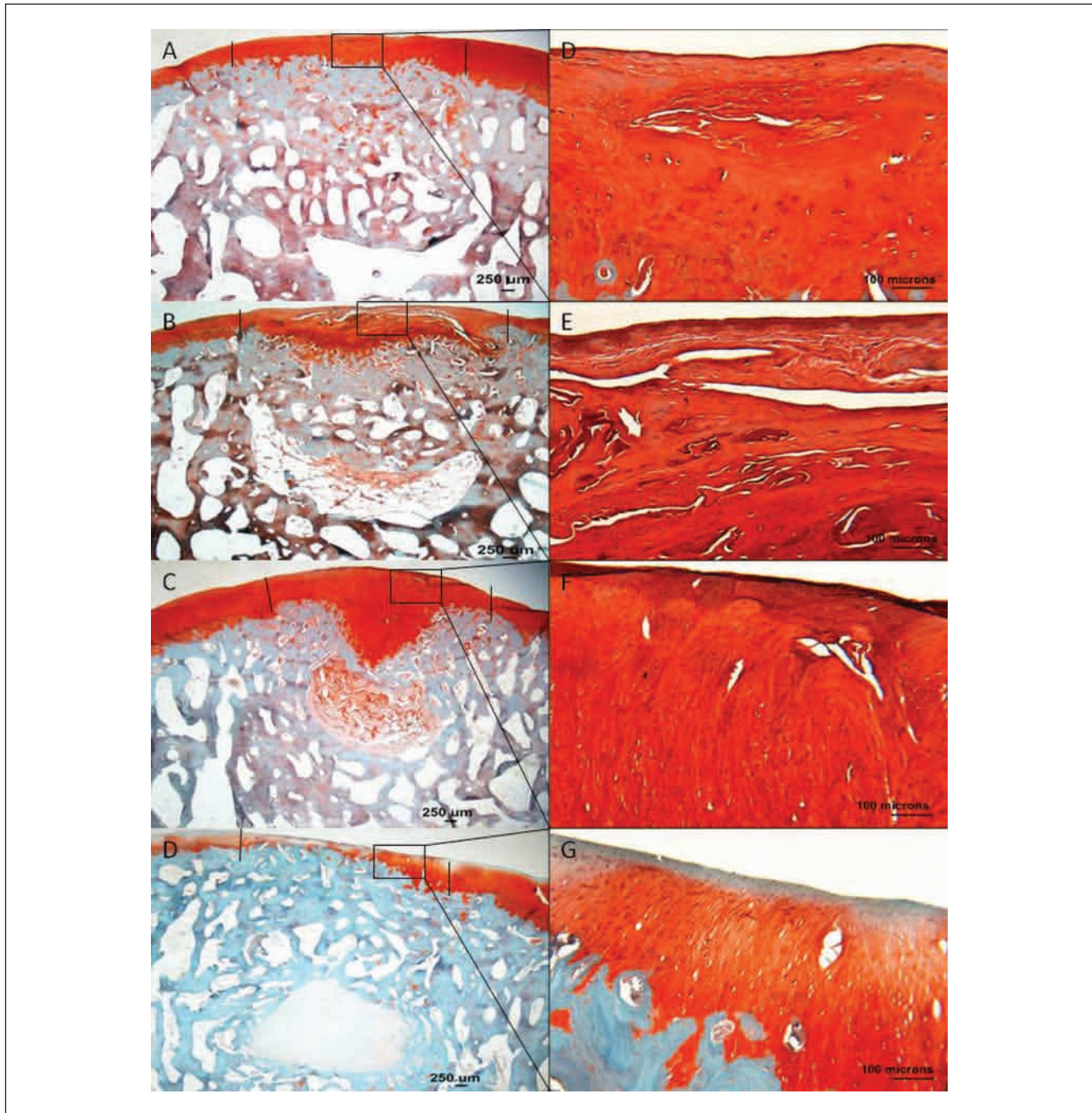


Figure 3. Histology sections stained with Safranin O/Fast Green, representing the median modified O'Driscoll scores of the MFC of treatment groups. (A and E) Empty defects, (B and F) scaffold only, (C and G) PRP + scaffold, and (D and H) scaffold + CBMA. (A-D) 1x magnification, and (E-H) 10x magnification. The edge of the defect is marked with a black line. Good lateral integration is seen in all the scaffold-filled defects. The thickness of the cartilage layer in the PRP group is nearly normal (C); however, a central cleft is noted. Strong Safranin O staining is noted within the PRP + scaffold ECM, with some evidence of organized tissue being produced.

suggestive of repair tissue with more characteristics of hyaline cartilage when PRP is loaded onto the biphasic scaffold prior to implantation into an osteochondral defect.

In addition to these effects on cartilage repair, the presence of autologous factors on the scaffold had an effect on

scaffold retention and cyst formation within subchondral bone. The presence of CBMA on the biphasic scaffold markedly reduced the amount of residual scaffold present in the lesion; that is, most of the scaffold had been resorbed at the 26-week time point. A further interesting finding was

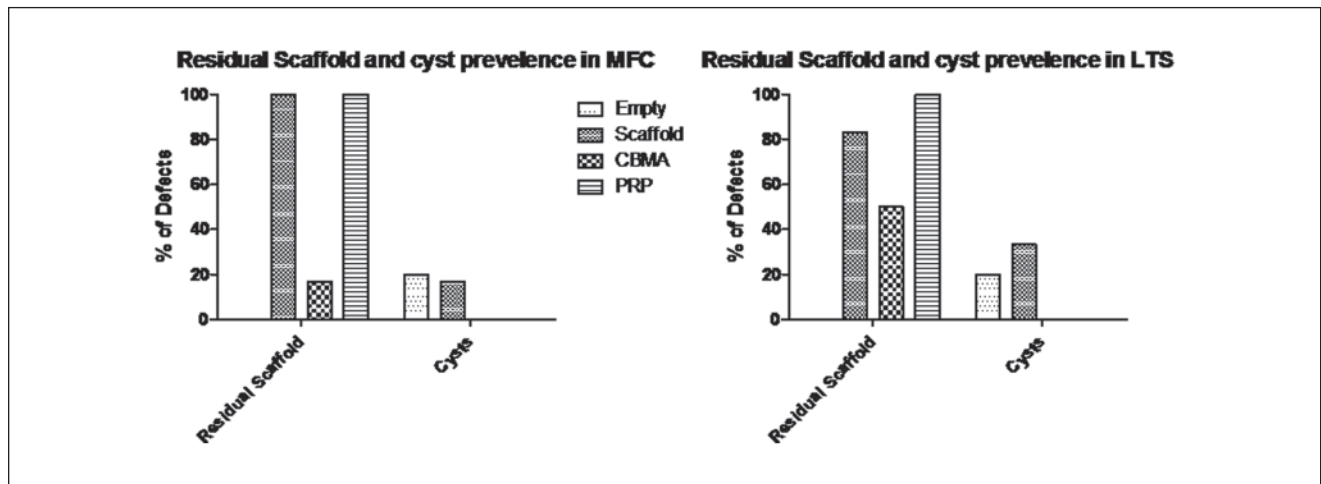


Figure 4. Residual scaffold and cyst formation in empty osteochondral defects (Empty), osteochondral defects filled with ChondroMimetic scaffold (Scaffold), osteochondral defects filled with ChondroMimetic scaffold loaded with concentrated bone marrow aspirate cells (CBMA), and osteochondral defects filled with ChondroMimetic scaffold loaded with platelet-rich plasma (PRP). Data are presented for defects in both the medial femoral condyle (MFC) and the lateral trochlea sulcus (LTS).

that, in the absence of a scaffold or with the scaffold alone, 22% of the lesions had a large cyst in the subchondral bone region compared to no cysts being detected in the presence of PRP or CBMA on the scaffold. Subchondral bone cysts are often detected in osteochondral repair models; in a similar caprine study, cysts were detected in 17% of scaffold only defects,¹¹ whereas in a sheep osteochondral autograft model, 60% of the operated defects developed cysts.²⁶ The mechanism by which cysts form is not fully known; however, it has been suggested that cyst formation in the osteochondral repair is secondary to synovial fluid pressure on the subchondral bone. It may be that the addition of CBMA or PRP may promote tissue fill in the cartilage defect area more quickly than occurs in empty defects or those filled with porous scaffold alone, effectively sealing off the subchondral bone from the synovial fluid more rapidly and decreasing cyst formation.

The mechanism by which PRP may be exerting an effect on cartilage repair tissue is not fully proven. Previous work in our group has demonstrated release of TGF- β 1, PDGF-AB, and FGF-2 from the biphasic scaffold used in this study.²² It is hypothesized that the effects of these growth factors may contribute to the formation of a more hyaline cartilage-like phenotype in the repair tissue observed in this study when PRP is included with the scaffold to assist repair of the osteochondral lesions. However, the effect of PRP upon osteochondral healing is clearly not fully understood, with limited studies being performed in large animal models. Kon *et al.* noted that the addition of PRP to a triphasic hydroxyapatite-collagen scaffold had a negative effect on osteochondral lesion repair in an ovine model²⁷; PRP induced a highly amorphous cartilage repair tissue with poorly organized subchondral bone. In a caprine

model, the use of PRP as an adjunct to autologous chondrocyte transplantation did not lead to improved results.²⁸ However, in an ovine microfracture model, adjunctive use of PRP produced repair tissue that was more histologically differentiated,²⁹ while in a small animal (rabbit) model, PRP has been shown to have a positive effect on osteochondral repair in combination with a polyglycolic scaffold.³⁰

One of the limits of using PRP at the current time is that the method of production and the product obtained are not standardized.^{29,31} In this study, both CBMA and PRP were prepared from the individual animal prior to scaffold loading and implantation, and marked individual variability in the product applied to the scaffold was noted. The range of cells present within the CBMA was between 0.25 to $6.87 \times 10^9/L$, while the range of platelet numbers in PRP was between 210 and $3,634 \times 10^9/L$ with a concentration range of between 3.0 and 33.9 times. As other authors have done, we performed a preliminary study prior to this pilot study to optimize the centrifugation required to provide a standard concentration of platelets; however, this was poorly achieved, despite this initial work. It has been suggested that the optimum platelet concentration required for maximum healing efficacy is 1 million platelets/ μL and that greater than this amount may lead to an inhibitory effect.³² There was some evidence that an inhibition effect may be occurring in the study reported here, with a negative correlation found between the platelet concentration factor and the O'Driscoll score in the LTS samples. However, despite concerns being raised in the literature as to the effect of leucocytes in the PRP preparations obtained from the currently available commercial preparatory systems,^{33,34} no correlation was found between leucocyte concentration and the osteochondral repair observed in this study.

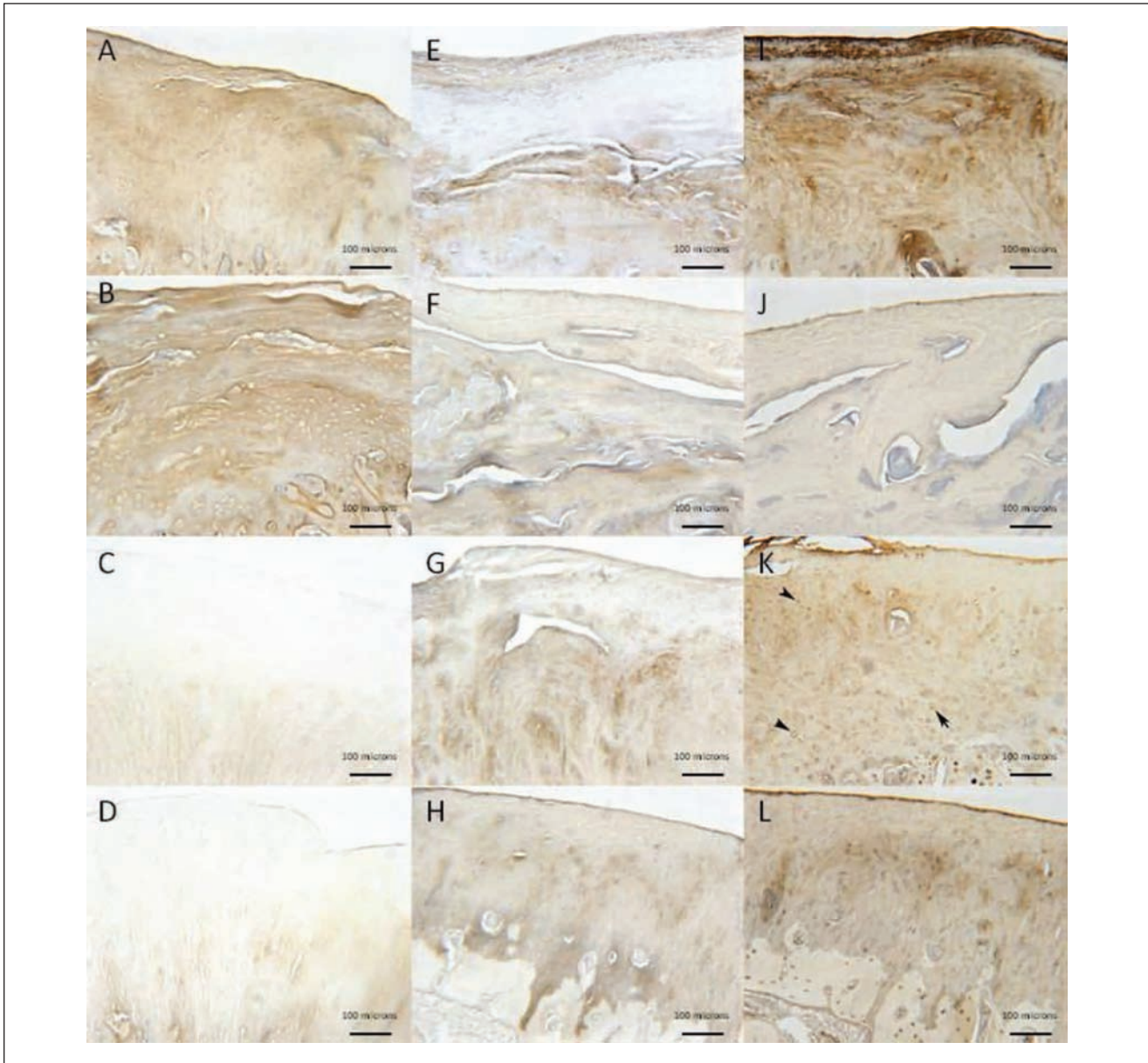


Figure 5. Immunolocalization in the MFC of collagen types I (**A-D**), II (**E-H**), and VI (**I-L**) for empty defects (**A**, **E**, and **I**), scaffold only (**B**, **F**, and **J**), PRP + scaffold (**C**, **G**, and **K**), and CBMA + scaffold (**D**, **H**, and **L**) (10x magnification). Positive staining is signified by the brown color. Positive type I staining is seen in the empty defect (**A**) and scaffold only (**B**) with limited type II staining (**E** and **F**, respectively). Improved type II staining is observed in the PRP group (**G**) with pericellular type VI staining (**K**, denoted by black arrowhead).

This pilot study does have some limitations in addition to the variability in the PRP obtained for application onto the scaffold. Firstly, healing within the empty defects was noted. In many cases, good defect fill with fibrocartilaginous repair tissue was seen, often with similar properties to the treatment groups. This observation does question whether the 5.8-mm osteochondral defects are of critical size. Jackson *et al.* have shown that a 6-mm defect is of critical size in the MFC of Spanish goats.³⁵ Osteochondral defects were made in the weightbearing portion of the MFC,

which did not spontaneously heal by 12 months after creation. These animals are of similar size and weight to the Welsh Mountain sheep used in this study, hence why an approximately 6-mm defect was chosen for this study. The width of the femoral condyle is a major determinant of the size of defect that can be made. If a larger defect than 6 mm were created, a significant alteration in topographic anatomy would be made to the condyle, and a likely marked change in tibiofemoral contact pressures would be established.³⁶ We therefore suggest that increasing the size of the

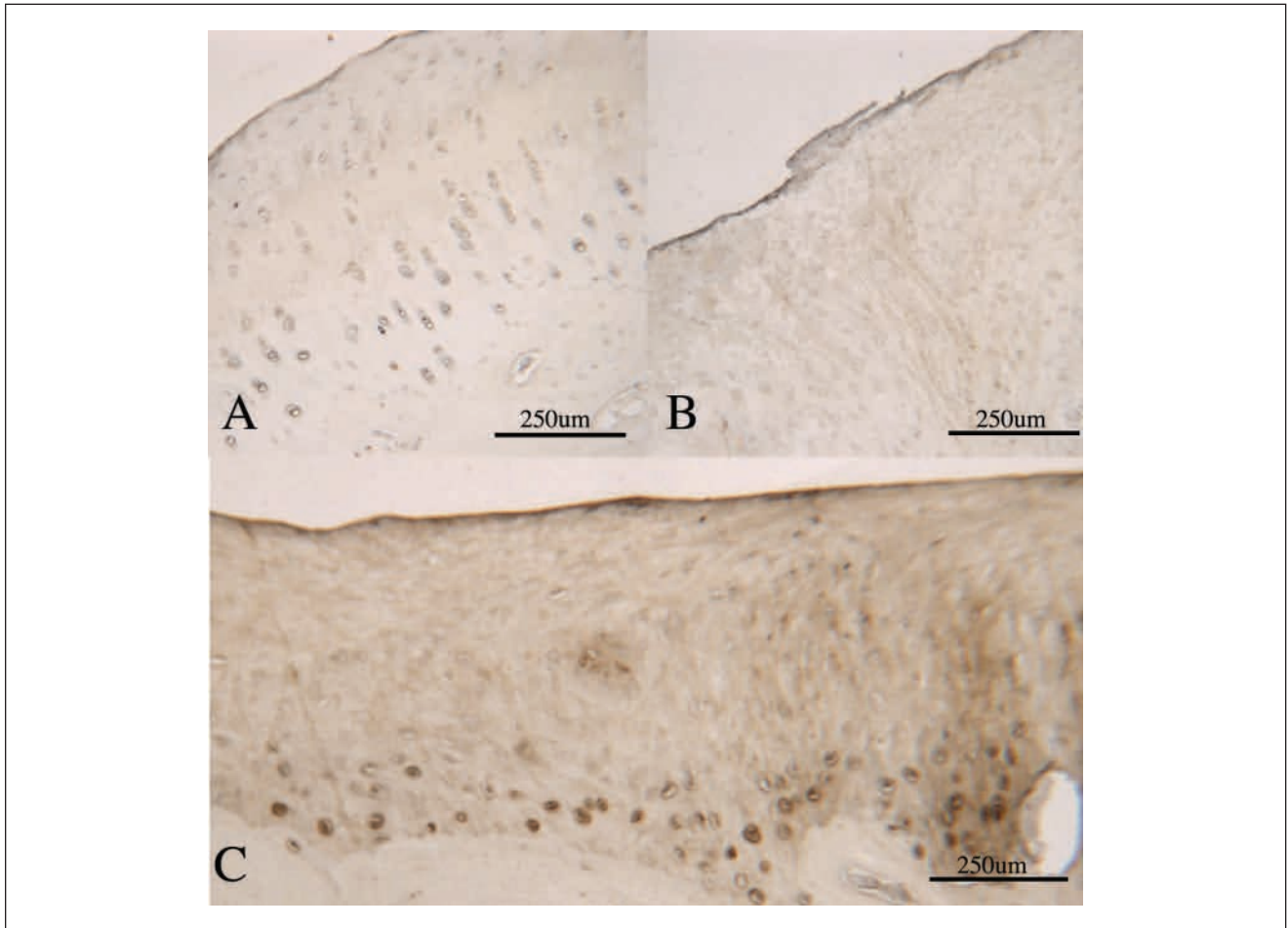


Figure 6. Photomicrographs demonstrating type VI collagen immunohistochemistry in repair tissue. **(A)** Type VI collagen staining in normal cartilage, adjacent to an osteochondral defect. Type VI collagen is seen as a pericellular halo around all the chondrocytes in the section. **(B)** Fibrocartilage repair within an osteochondral defect: there is no pericellular type VI collagen present, indicating a lack of maturity of the chondrocytes in the repair tissue. **(C)** A mixed hyaline/fibrocartilage repair within an osteochondral defect. In this section, there is strong pericellular type VI collagen staining associated with the chondrocytes in the deep zone, adjacent to the subchondral bone (dark stained cells), indicating that these cells are mature hyaline chondrocytes. In the overlying, more poorly organized tissue, there is no pericellular staining, indicating a lack of maturity in these chondrocytes.

defect could not only be detrimental to the repair tissue but also the perilesional cartilage as well. However, even if this 5.8-mm defect is considered as below the critical size for an osteochondral defect at this site, the observation that neither PRP nor CBMA applied to a biphasic scaffold could assist with the healing, as measured by a number of quantitative assessments, is even stronger evidence that these factors are not beneficial in tissue healing at this site, even in lesions that are small enough to require no healing assistance.

A second limitation of this study was that the quality of the repair was only assessed at 26 weeks, when the lesions were not fully healed. It may be hypothesized that healing would be more advanced at a later time point and that a more accurate comparison between treatment groups could be made.

In conclusion, the results of this pilot study suggest that the addition of CBMA combined with a collagen-GAG

biphasic scaffold shows no benefit over an empty 5.8-mm osteochondral defect or a defect filled with the scaffold alone apart from a reduction in subchondral cyst formation. The addition of PRP/scaffold to the defect did not improve tissue repair, as measured by quantitative assessment, but showed evidence of a more hyaline-like cartilage repair tissue in the defect and a reduction in subchondral cyst formation. Given that PRP is a cheap, readily available biologic, we would suggest that it merits further investigation in a larger large animal trial, possibly with an extended period of study of up to 52 weeks.

Acknowledgments and Funding

The authors acknowledge research grant funding support from the UK Technology Strategy Board, TiGenix Ltd. (Cambridge, UK), and the NIHR.

Declaration of Conflicting Interests

The author(s) declared the following potential conflicts of interest with respect to the research, authorship, and/or publication of this article: Two of the authors (A.G., N.R.) receive consultancy fees from TiGenix Ltd. L.A.F. receives institutional research support from Harvest Technologies Inc. None of the other authors have any conflict of interest to declare.

References

1. Bedi A, Feeley BT, Williams RJ III. Management of articular cartilage defects of the knee. *J Bone Joint Surg Am*. 2010;92:994-1009.
2. Steadman JR, Rodkey WG, Rodrigo JJ. Microfracture: surgical technique and rehabilitation to treat chondral defects. *Clin Orthop Relat Res*. 2001;(391 Suppl):S362-9.
3. Brittberg M, Lindahl A, Nilsson A, Ohlsson C, Isaksson O, Peterson L. Treatment of deep cartilage defects in the knee with autologous chondrocyte transplantation. *N Engl J Med*. 1994;331:889-95.
4. Hangody L, Kish G, Karpati Z, Szerb I, Udvarhelyi I. Arthroscopic autogenous osteochondral mosaicplasty for the treatment of femoral condylar articular defects: a preliminary report. *Knee Surg Sports Traumatol Arthrosc*. 1997;5:262-7.
5. Getgood A, Brooks R, Fortier L, Rushton N. Articular cartilage tissue engineering: today's research, tomorrow's practice? *J Bone Joint Surg Br*. 2009;91:565-76.
6. Gomoll AH, Madry H, Knutsen G, van DN, Seil R, Brittberg M, *et al*. The subchondral bone in articular cartilage repair: current problems in the surgical management. *Knee Surg Sports Traumatol Arthrosc*. 2010;18:434-47.
7. Kerker JT, Leo AJ, Sgaglione NA. Cartilage repair: synthetics and scaffolds. Basic science, surgical techniques, and clinical outcomes. *Sports Med Arthrosc*. 2008;16:208-16.
8. Swieszkowski W, Tuan BH, Kurzydowski KJ, Huttmacher DW. Repair and regeneration of osteochondral defects in the articular joints. *Biomol Eng*. 2007;24:489-95.
9. Harley BA, Lynn AK, Wissner-Gross Z, Bonfield W, Yannas IV, Gibson LJ. Design of a multiphase osteochondral scaffold, II: fabrication of a mineralized collagen-glycosaminoglycan scaffold. *J Biomed Mater Res A*. 2010;92:1066-77.
10. Lynn AK, Best SM, Cameron RE, Harley BA, Yannas IV, Gibson LJ, *et al*. Design of a multiphase osteochondral scaffold, I: control of chemical composition. *J Biomed Mater Res A*. 2010;92:1057-65.
11. Getgood AM, Kew SJ, Brooks R, Aberman H, Simon T, Lynn AK, *et al*. Evaluation of early-stage osteochondral defect repair using a biphasic scaffold based on a collagen-glycosaminoglycan biopolymer in a caprine model. *Knee*. Epub 2011 May 25.
12. Csaki C, Schneider PR, Shakibaei M. Mesenchymal stem cells as a potential pool for cartilage tissue engineering. *Ann Anat*. 2008;190:395-412.
13. Pittenger MF, Mackay AM, Beck SC, Jaiswal RK, Douglas R, Mosca JD, *et al*. Multilineage potential of adult human mesenchymal stem cells. *Science*. 1999;284:143-7.
14. Fortier LA, Potter HG, Rickey EJ, Schnabel LV, Foo LF, Chong LR, *et al*. Concentrated bone marrow aspirate improves full-thickness cartilage repair compared with microfracture in the equine model. *J Bone Joint Surg Am*. 2010;92:1927-37.
15. Wang W, Li B, Yang J, Xin L, Li Y, Yin H, *et al*. The restoration of full-thickness cartilage defects with BMSCs and TGF-beta 1 loaded PLGA/fibrin gel constructs. *Biomaterials*. 2010;31:8964-73.
16. Sauerbier S, Stricker A, Kuschnierz J, Buhler F, Oshima T, Xavier SP, *et al*. In vivo comparison of hard tissue regeneration with human mesenchymal stem cells processed with either the FICOLL method or the BMAC method. *Tissue Eng Part C Methods*. 2010;16:215-23.
17. Alsousou J, Thompson M, Hulley P, Noble A, Willett K. The biology of platelet-rich plasma and its application in trauma and orthopaedic surgery: a review of the literature. *J Bone Joint Surg Br*. 2009;91:987-96.
18. Oprea WE, Karp JM, Hosseini MM, Davies JE. Effect of platelet releasate on bone cell migration and recruitment in vitro. *J Craniofac Surg*. 2003;14:292-300.
19. van den DJ, Mooren R, Vloon AP, Stoeltinga PJ, Jansen JA. Platelet-rich plasma: quantification of growth factor levels and the effect on growth and differentiation of rat bone marrow cells. *Tissue Eng*. 2006;12:3067-73.
20. Akeda K, An HS, Okuma M, Attawia M, Miyamoto K, Thonar EJ, *et al*. Platelet-rich plasma stimulates porcine articular chondrocyte proliferation and matrix biosynthesis. *Osteoarthritis Cartilage*. 2006;14:1272-80.
21. Drengk A, Zapf A, Sturmer EK, Sturmer KM, Frosch KH. Influence of platelet-rich plasma on chondrogenic differentiation and proliferation of chondrocytes and mesenchymal stem cells. *Cells Tissues Organs*. 2009;189:317-26.
22. Getgood A, Henson F, Brooks R, Fortier LA, Rushton N. Platelet-rich plasma activation in combination with biphasic osteochondral scaffolds-conditions for maximal growth factor production. *Knee Surg Sports Traumatol Arthrosc*. 2011;19:1942-7.
23. Frenkel SR, Bradica G, Brekke JH, Goldman SM, Ieska K, Issack P, *et al*. Regeneration of articular cartilage: evaluation of osteochondral defect repair in the rabbit using multiphasic implants. *Osteoarthritis Cartilage*. 2005;13:798-807.
24. Hosgor M, Karaca I, Ozer E, Suzek D, Ulukus C, Ozdamar A. Do alterations in collagen synthesis play an etiologic role in childhood inguinoscrotal pathologies: an immunohistochemical study. *J Pediatr Surg*. 2004;39:1024-9.
25. Loeser RF. Growth factor regulation of chondrocyte integrins: differential effects of insulin-like growth factor 1 and transforming growth factor beta on alpha 1 beta 1 integrin expression and chondrocyte adhesion to type VI collagen. *Arthritis Rheum*. 1997;40:270-6.

26. Benazzo F, Cadossi M, Cavani F, Fini M, Giavaresi G, Setti S, *et al.* Cartilage repair with osteochondral autografts in sheep: effect of biophysical stimulation with pulsed electromagnetic fields. *J Orthop Res.* 2008;26:631-42.
27. Kon E, Delcogliano M, Filardo G, Fini M, Giavaresi G, Francioli S, *et al.* Orderly osteochondral regeneration in a sheep model using a novel nano-composite multilayered bio-material. *J Orthop Res.* 2010;28:116-24.
28. Brehm W, Aklin B, Yamashita T, Rieser F, Trub T, Jakob RP, *et al.* Repair of superficial osteochondral defects with an autologous scaffold-free cartilage construct in a caprine model: implantation method and short-term results. *Osteoarthritis Cartilage.* 2006;14:1214-26.
29. Milano G, Sanna PE, Deriu L, Careddu G, Manunta L, Manunta A, *et al.* The effect of platelet rich plasma combined with microfractures on the treatment of chondral defects: an experimental study in a sheep model. *Osteoarthritis Cartilage.* 2010;18:971-80.
30. Sun Y, Feng Y, Zhang CQ, Chen SB, Cheng XG. The regenerative effect of platelet-rich plasma on healing in large osteochondral defects. *Int Orthop.* 2010;34:589-97.
31. Everts PA, Brown MC, Hoffmann JJ, Schonberger JP, Box HA, van ZA, *et al.* Platelet-rich plasma preparation using three devices: implications for platelet activation and platelet growth factor release. *Growth Factors.* 2006;24:165-71.
32. Weibrich G, Hansen T, Kleis W, Buch R, Hitzler WE. Effect of platelet concentration in platelet-rich plasma on peri-implant bone regeneration. *Bone.* 2004;34:665-71.
33. Everts PA, Hoffmann J, Weibrich G, Mahoney CB, Schonberger JP, van ZA, *et al.* Differences in platelet growth factor release and leucocyte kinetics during autologous platelet gel formation. *Transfus Med.* 2006;16:363-8.
34. Zimmermann R, Reske S, Metzler P, Schlegel A, Ringwald J, Eckstein R. Preparation of highly concentrated and white cell-poor platelet-rich plasma by plateletpheresis. *Vox Sang.* 2008;95:20-5.
35. Jackson DW, Lalor PA, Aberman HM, Simon TM. Spontaneous repair of full-thickness defects of articular cartilage in a goat model: a preliminary study. *J Bone Joint Surg Am.* 2001;83-A:53-64.
36. Guettler JH, Demetropoulos CK, Yang KH, Jurist KA. Osteochondral defects in the human knee: influence of defect size on cartilage rim stress and load redistribution to surrounding cartilage. *Am J Sports Med.* 2004;32:1451-8.